

Criticality of Exothermic Chemical Reactions: the Role of Reaction Barrier

Qun-Li Lei,¹ Hao Hu,² and Ran Ni^{1,*}

¹*School of Chemical and Biomedical Engineering,*

Nanyang Technological University, 62 Nanyang Drive, 637459, Singapore

²*School of Physics and Materials Science, Anhui University, Hefei 230601, China*

The critical behavior of exothermic chemical reactions is of not only fundamental significance, but also practical relevance in chemical engineering and energy/engine industries. Here, using computer simulation and theoretical analysis, we study the effect of reaction barrier on the criticality of dynamic phase transitions in a minimal reactive hard-sphere model. At zero thermal temperature limit, with increasing the reaction barrier, the type of transition changes from a continuous conserved directed percolation into a discontinuous dynamic transition by crossing a tricritical point. A mean-field theory is proposed to explain this phenomenon, which suggests that the transition at finite temperature belongs to the Ising universality. Moreover, we obtain the tricritical exponents in the systems which quantitatively agree with field theory simulations. This mechanism of barrier-control criticality also has implications in epidemic spreading and dynamic network systems.

PACS numbers:

Chemical reactions can be either mild processes like oxidative rusting, or catastrophic ones, like combustion, which reflects different reaction rates. In some exothermic chemical reactions, the reaction rate can be self-accelerated and jump abruptly resulting in the thermal explosion [1]. In 1920s, Semenov proposed the first theory of thermal explosion, i.e., the celebrated Semenov model, which assumes a uniform temperature distribution and neglects the reactant consumption at the ignition [2]. Despite several important modifications done by Frank-Kamenetskii and many other chemists [1, 3–5], this model is still the starting point to study the criticality of chemical reactions [6–9]. Nevertheless, from the perspective of physics, exothermic chemical reactions are complex dynamic phase transitions. Currently, dynamic critical phenomena have been only studied in some specific chemical reaction systems [10–15], e.g., the Schlogl’s first and second models [10]. However, due to the specificity of reactants, the influence of reactant consumption/reaction product, heat transfer and thermal fluctuations, etc. [9, 16–19], it remains unclear whether there is any general physical law controlling the criticality of exothermic chemical reactions.

Recently, in statistical physics, it was found that the continuous percolation transition can be tuned to an explosive transition [20–23]. The physics behind this phenomenon was later summarised to a delaying mechanism that sharpens the transition [24]. This raises a question whether a similar mechanism exists in chemical reactions. To this end, we propose a minimal reactive hard-sphere model in the spirit of Semenov model. By using simulation and theory, we prove that the reaction barrier controls the criticality or “sharpness” of exothermic chemical reactions: at zero thermal temperature, increasing the reaction barrier changes the type of reaction transition from a continuous conserved directed percolation (CDP) [25, 26] to a discontinuous dynamic transition by

crossing a tricritical point, while at finite thermal temperature, the transition becomes Ising-type.

The model we consider can be viewed as a generalization of the Semenov model with neglected reactant consumption [26]. It consists of N reactive hard spheres with the same mass m and diameter σ . The dimensionality of the system is $d=2,3$ with periodic boundary conditions in all directions. The reduced particle density of the system is defined as $\bar{\rho}=N\sigma^d/V$ with $V=L^d$ the volume of the system and L the box length. Reactions occur in pairwise collisions between two particles, if their relative kinetic energy along the center-to-center direction surpass the reaction barrier E_b . During each reaction, an energy ϵ is released in the center-to-center direction, with the momentum of the two particles conserved [26]. The typical excitation speed is defined as $v_0=\sqrt{\epsilon/m}$, and the time unit of the system is set as $\tau_0=\sigma/v_0$. The equation of motion for particle i between two consecutive collisions is

$$m \frac{d\mathbf{v}_i(t)}{dt} = -\gamma \mathbf{v}_i(t) + \sqrt{2\gamma k_B T} \eta(t), \quad (1)$$

where γ is the damping coefficient, which may result from the solvent, non-reactants, substrate, or the boundary in dilute confined system [6, 7]. Based on the fluctuation-dissipation theorem, γ is also associated with the second noise term with T the thermal temperature and $\eta(t)$ the Gaussian white noise. The typical dissipation time for each reaction is $\tau_d=m/\gamma$. We adopt an event-driven algorithm [26, 27] to simulate the system in both 2D and 3D.

We first study the 2D system at $T=0$. In this case, as shown in Ref [26], there are two important characteristic lengths in the system, i.e., the mean free path l_m and the dissipation length $l_d=\sqrt{m\epsilon}/\gamma$. The later is the typical distance that isolated particles can travel after a single reaction. With increasing the ratio of l_d/l_m , the system undergoes a dynamic absorbing-active phase transition at

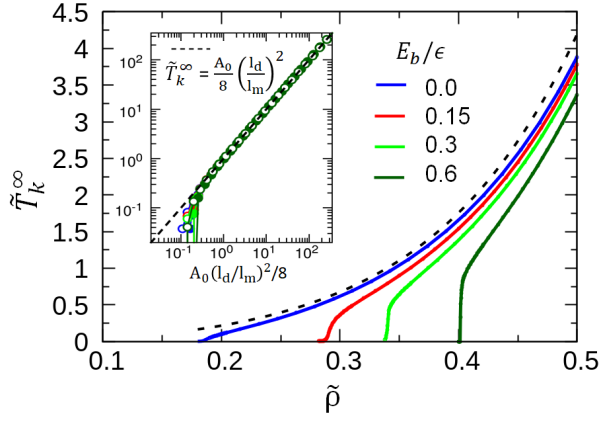


FIG. 1: \tilde{T}_k^∞ as a function of density for 2D system with different E_b . Inset: \tilde{T}_k^∞ as a function of l_d ($\tilde{\rho}=0.1$) and l_m ($l_d=160\sigma$). The dashed lines are the theoretical predictions with $A_0=1.56$.

$l_d \simeq l_m$ [26]. Here, the absorbing state corresponds to zero kinetic energy state while the active state has a positive kinetic temperature. Thus, the order parameter of the system can be chosen as the reduced kinetic temperature of the system, i.e.,

$$\tilde{T}_k(t) = \frac{dk_B T_k(t)}{\epsilon} \quad \text{and} \quad k_B T_k(t) = \frac{m \langle \overline{v^2}(t) \rangle}{d}, \quad (2)$$

Here, $\overline{v^2}$ is average square of speed of all particles and the $\langle \cdot \rangle$ calculates the ensemble average of active (surviving) trials [28]. In Fig. 1, we plot \tilde{T}_k as a function of density for systems with different reaction barriers. With increasing E_b , the transition shifts to higher density regime and becomes sharper, similar to the explosive percolation [20–23]. To determine the types of the transitions, we assume there is a scaling-invariant critical point $\tilde{\rho}_c$ in the system and perform finite-size analysis to determine $\tilde{\rho}_c$ and the corresponding critical exponents. For systems near the critical point, the saturated kinetic temperature $\tilde{T}_k^\infty(\Delta\tilde{\rho}, L)$ satisfies the scaling relationship [12, 28],

$$\tilde{T}_k^\infty(\Delta\tilde{\rho}, L) = L^{-\beta/\nu_\perp^*} \mathcal{G}\left(L^{1/\nu_\perp^*} \Delta\tilde{\rho}\right), \quad (3)$$

where $\Delta\tilde{\rho} = \tilde{\rho} - \tilde{\rho}_c$ and $\mathcal{G}(\cdot)$ is the scaling function. For systems at the critical point ($\Delta\tilde{\rho}=0$), starting from random initial configurations, $\tilde{T}_k(t)$ follows a power-law decay $t^{-\alpha}$ before reaching the saturated value satisfying $\tilde{T}_k^\infty \sim L^{-\beta/\nu_\perp^*}$. In Fig. 2a, we show the decay of $\tilde{T}_k(t)$ for a 2D system of different size $L \propto N^{1/d}$ for $E_b=0$ and $l_d=2\sigma$. The inset plots \tilde{T}_k^∞ as a function of L . Both figures indicate the scaling-invariance and we obtain the corresponding critical exponents $\alpha=0.54$ and $\beta/\nu_\perp^*=-0.77$. In Fig. 2d, we plot the collapse of $\tilde{T}_k^\infty(\Delta\tilde{\rho}, L)$ for difference L (solid symbols) based on Eq. (3) with $\beta=0.64$ and $\nu_\perp^*=0.84$, which is consistent with the obtained β/ν_\perp^* . We also use another similar finite-size scaling methods to obtain $z=1.50$ (See SI and Fig. S1 for details). These

exponents for $E_b=0$ are summarized in Table I, which indicates that the universality of this phase transition belongs to the conserved directed percolation (CDP) or Manna class [25, 26]. Nevertheless, with a similar analysis for systems of $E_b=0.165\epsilon$ in Fig. 2b,d, and Fig. S2, we obtain critical exponents distinct from CDP (Table I). As shown later, these unreported exponents appear because the system is at a tricritical point, which separates the continuous and discontinuous transitions. Indeed, by further increasing E_b to 0.3ϵ , we find the finite-size scaling breaks down and the system exhibits the bistability at $k_B T = 0.02\epsilon$ (Fig. 2c), indicating the system undergoes a discontinuous transition at large reaction barrier even with a finite thermal noise. This result is consistent with the previous findings by chemists, i.e., decreasing the reaction barrier can make the reaction from explosion to slow combustion [29–31].

To determine the tricritical point, we employ a crossover scaling analysis [32–34]. Supposing $E_{b,c}$ is the tricritical energy barrier and letting $\Delta E_b = E_b - E_{b,c}$, the crossover scaling can be written as

$$\tilde{T}_k(\Delta\tilde{\rho}, \Delta E_b) = \Delta E_b^{-\beta_t/\phi} \mathcal{G}_t(\Delta\tilde{\rho} \Delta E_b^{-1/\phi}), \quad (4)$$

providing $\Delta\tilde{\rho} \ll \Delta E_b/\epsilon$ [32]. Here, the scaling function $\mathcal{G}_t(x) \sim x^\beta$ when $x \ll 1$ and $\mathcal{G}_t(x) \sim x^{\beta_t}$ when $x \gg 1$ with β_t the tricritical exponent. In Fig. 2e, we show the collapse of $\tilde{T}_k(\Delta\tilde{\rho})$ for systems with different E_b (solid symbols), which leads to $E_{b,c}=0.165\epsilon$ and $\phi=0.32$.

	$\beta_{(t)}$	α	ν_\perp^*	z^*	ϕ
CDP	0.64(1)	0.52(1)	0.80(2)	1.53(2)	
$E_b=0$	0.64(2)	0.54(2)	0.84(3)	1.50(3)	
$b=1$	0.65(2)	0.53(2)	0.84(3)	1.51(2)	
$E_b = E_{b,c}$	0.32(4)	0.37(5)	0.68(4)	1.68(5)	0.32(5)
$b = b_c$	0.33(3)	0.36(4)	0.70(3)	1.65(5)	0.34(4)

TABLE I: Comparison of critical exponents in 2D systems. Data for CDP is from [12, 35]. Different values of E_b and b are for reactive hard-sphere model and field simulations, respectively. Tricritical points are at $E_{b,c}=0.165(5)\epsilon$ and $b_c=-0.92(3)$.

Next we formulate an analytical theory to explain the above complex phase behavior. As a generalization from [26], at the mean-field level, the reaction driving power per particle is $W_{driv} = f_a \epsilon$ and the dissipation power is $W_{disp} = \overline{v^2} \gamma$. Here, $f_a = x_a \bar{v}_a / (2l_r)$ is the average reactive collision frequency per particle with l_r the mean free path of reactive collisions, which equals l_m at $E_b=0$. x_a is the fraction of activated particles and \bar{v}_a is the average speed of activated particle. Moreover, the driving power of thermal noise per particle W_{driv}^{therm} can be approximated by the equilibrium dissipation power $W_{disp}^{therm} = \gamma dk_B T / m$. Thus, the dynamic equation for ki-

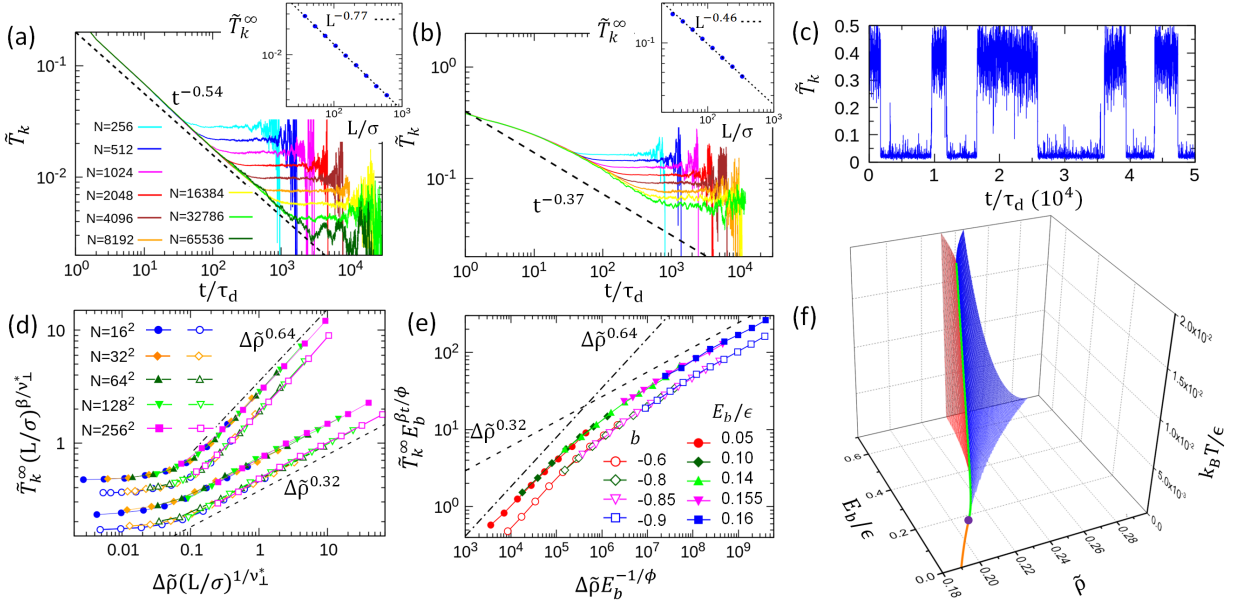


FIG. 2: (a,b) \tilde{T}_k as a function of t for different system sizes with inset showing saturated value as a function of system size. (a) $E_b=0$, $\tilde{\rho}=0.18471$; (b) $E_b=0.165\epsilon$, $\tilde{\rho}=0.29615$. (c) Demonstration of bistability at $E_b=0.3\epsilon$, $\tilde{\rho}=0.3290$ with thermal noise $k_B T=0.02\epsilon$ for a system with $N=1024$. (d) Collapse of $\tilde{T}_k(\Delta\tilde{\rho})$ according to Eq. (3) for different system sizes. Solid symbols are for reactive hard-sphere systems with $E_b=0.0$ (upper), 0.165ϵ (lower), respectively. The open symbols obtained in field simulations with $b=1$ (upper), -0.92 (lower), respectively. (e) Crossover scaling analysis of the tricritical point based on Eq (4). (f) Phase diagram of the mean-field theory using $A=0.095$, $B=1/2$ and $\tau_d/\tau_0=10$. The orange line and green line represent of the CDP and Ising-type critical points of the system, respectively. The purple point is the tricritical point. The bistability region is enclosed by the blue and red surfaces.

netic energy per particle can be written as

$$\begin{aligned} \epsilon \frac{\partial \tilde{T}_k}{\partial t} &= W_{driv} - W_{disp} + W_{driv}^{therm} \\ &= \frac{x_a \tilde{\rho}_r \bar{v}_a \epsilon}{2\sigma} - \gamma \bar{v}^2 + \frac{\gamma dk_B T}{m} \end{aligned} \quad (5)$$

Here we use the low density approximation $l_r \simeq \sigma/\tilde{\rho}_r$ with $\tilde{\rho}_r$ the density of reactant. For systems at $T=0$ far from the critical point ($l_d \gg l_m$ and $\tilde{T}_k \gg E_b/\epsilon$), we have $\tilde{\rho}_r \simeq \tilde{\rho}$, $x_m \simeq 1$ and $\bar{v}_a \simeq \bar{v}$ with \bar{v} the average speed of all particles. Based on the approximation $\bar{v}^2 \simeq \bar{v}^2 = dk_B T/m$, the steady-state \tilde{T}_k can be obtained as $\tilde{T}_k^\infty \simeq \frac{1}{4d} \left(\frac{l_d}{l_m} \right)^2$, which does not depend on E_b . This independence is verified in simulations as shown in the inset of Fig. 1. Nevertheless, for systems close to the critical point, there is strong dynamic heterogeneity, i.e., most particles are immobile and only a small fraction of particles are activated with average speed $\bar{v}_a \simeq v_0$. Apparently, \bar{v}_a is a convex instead of concave function of x_a , since increasing x_a increases the collision between excited particles, further raising \bar{v}_a . Thus, as a first-order approximation, we have

$$\bar{v} \simeq (1 + Ax_a)v_0 \quad (6)$$

$$\tilde{T}_k \simeq x_a m \bar{v}_a^2 / \epsilon \simeq x_a + 2Ax_a^2 \quad (7)$$

with the coefficient $A > 0$ indicating the convexness. Accordingly, we can rewrite x_a as a function of order pa-

rameter \tilde{T}_k :

$$x_a \simeq \tilde{T}_k - 2A\tilde{T}_k^2. \quad (8)$$

Moreover, for systems with $E_b > 0$, one can expect that there would be a fraction of collisions between active and inactive particles that do not induce reactions. This effect leads to the decrease of reactant density. therefore, as a first-order approximation, we can have

$$\tilde{\rho}_r / \tilde{\rho} = 1 - B(1 - x_a)\tilde{E}_b \quad (9)$$

with the coefficient $B > 0$. Finally, by keeping only the first three leading terms, Eq. (5) can be written as

$$\frac{\partial \tilde{T}_k}{\partial \tilde{t}} = a\tilde{T}_k - b\tilde{T}_k^2 - c\tilde{T}_k^3 + h \quad (10)$$

with $\tilde{t} = t/\tau_0$, $h = \gamma\tau_0 dk_B T / (m\epsilon)$ and

$$a = \frac{\tilde{\rho}}{2}(1 - B\tilde{E}_b) - \frac{\tau_0}{\tau_d} \quad (11)$$

$$b = -\frac{\tilde{\rho}}{2} \left[(1+A)B\tilde{E}_b - A \right] \quad (12)$$

$$c = \frac{\tilde{\rho}}{2} \left[4A^2 + (3A - 4A^2)B\tilde{E}_b \right] \quad (13)$$

The solution of this cubic dynamic equation is given in SI. The phase diagram of Eq. (10) is summarized in Fig. 2f. In the cases of zero thermal temperature ($T=0$) and $E_b < E_{b,c}$ (or $b > 0$), Eq.(10) has only one fixed point at

$a=0$ and the systems undergo a continuous phase transition with mean-field critical exponent $\beta_{\text{MF}}=1$ and upper critical dimension $d_c=4$. The transition points are shown as an orange curve in Fig. 2f. In contrast, when E_b increases above $E_{b,c}$ (or $b<0$), Eq.(10) has two fixed points, which corresponds to a bistability or a discontinuous dynamic phase transition. Importantly, $E_b=E_{b,c}$ (or $b=0$) is the tricritical point with $\beta_{\text{MF}}=1/2$ and $d_c=3$, which separates the continuous and discontinuous phase transitions (purple point in Fig. 2f). In the presence of thermal noise ($T>0$), the continuous phase transition is meshed out accompanied by the shrink of bistability region (enclosed by red and blue surfaces). This general picture is insensitive to the specific choice of coefficients A, B and agrees qualitatively with the simulation results.

We further go beyond the mean-field level by cooperating spatial-temporal fluctuations in the theory. In this scenario, the local temperature field $\tilde{T}_k^l(\mathbf{r}, t)$ is coupled with the local density field $\tilde{\rho}_l(\mathbf{r}, t)$, and,

$$\frac{\partial \tilde{T}_k^l}{\partial t} = a\tilde{T}_k^l - b\tilde{T}_k^{l2} - c\tilde{T}_k^{l3} + \lambda \nabla^2 \tilde{T}_k^l - h + \Lambda \sqrt{\tilde{T}_k^l} \eta(\mathbf{r}, t) \quad (14)$$

$$\frac{\partial \tilde{\rho}_l}{\partial t} = D \nabla^2 \tilde{T}_k^l, \quad (15)$$

where, a, b, c are functions of $\tilde{\rho}_l(\mathbf{r}, t)$ based on Eq. (11-13). The last term in Eq. (14) represents the spatial-temporal fluctuation with Λ the noise magnitude. The second dynamic equation (Eq. (15)) is the thermophoretic diffusion equation. Eq. (14-15), in fact, share the same formula as in the Reggeon-field theory of CDP [36]. Since the criticality of dynamic equations does not depend on specific choice of parameters, the critical exponents for Eq. (14-15) should be the same as the standard Reggeon field theory in which b and $\tilde{\rho}$ are the controlling parameters with $a=a'\tilde{\rho}_l(\mathbf{r}, t)-a_0$. Other parameters are simply set as $a_0=1$, $a'=1$, $c=1$, $D=1$, $\Lambda=1$ [36]. Since the noise term is multiplicative, we adopt a numerical method based on Fokker-Planck equation [37] to integrate the standard Reggeon fields equations on square or cubic lattices. This method has been used to obtain the accurate critical exponent for both directed percolation and CDP [37], but not for the tricritical points. In Fig. 2d,e, the open symbols show the results from the field system simulations, which behave essentially the same as the reactive hard-sphere system. The obtained (tri)critical exponents are also given in Table I, which are consistent with those from the hard-sphere systems. Moreover, the upper critical dimension $d_c=3$ at tricriticality is also confirmed both in hard sphere systems and field simulations (see Fig. S3-S6 and Table S1).

Lastly, our theory predicts another critical line (the green line in Fig. 2f) in the finite thermal temperature regime ($T>0$), which satisfies $[a_c, b_c, \tilde{T}_{k,c}] = [-3(\frac{h}{c})^{2/3}, -3(\frac{h}{c})^{1/3}, (\frac{h}{c})^{1/3}]$. The universality of similar noise-induced critical points has been under debate

for a long time, first initiated by the Schlogl's second model [13–15, 38–40], later extended into dynamic network model [41–43]. In the following, we provide a new theoretical argument which suggests that this critical line belongs to the Ising universality. The core of this argument is that round the critical point $[a_c, b_c]$, we can find a direction in the (a, b) parameter space, i.e., $(\tilde{T}_{k,c}, 1)$, along which Eq.(10) can be rewritten as

$$\frac{\partial \Delta \tilde{T}_k}{\partial t} \simeq -c \Delta \tilde{T}_k (\Delta \tilde{T}_k^2 + \Delta b \tilde{T}_{k,c}/c), \quad (16)$$

with $\Delta \tilde{T}_k = \tilde{T}_k - \tilde{T}_{k,c}$ and $\Delta b = b - b_c$. Therefore, for $\Delta b < 0$, the system has two stable fix points $\Delta \tilde{T}_k \simeq \pm \sqrt{-\Delta b \tilde{T}_{k,c}/c}$, which indicates $\beta_{\text{MF}}=1/2$, consistent with the Ising universality. More importantly, Eq. (16) has Z_2 symmetry under the transformation $(\Delta \tilde{T}_k \rightarrow -\Delta \tilde{T}_k)$, another evidence for the Ising type. It should be noted that our conclusion is different from a recent theoretical work of dynamic network model [42, 43], in which the authors only did the perturbation along the orthogonal directions $(1, 0)$ and $(0, 1)$ and obtained $\beta_{\text{MF}}=1/3$. Accordingly, the authors concluded a DP-type univ ersality for this transition. In fact, systems described by the above cubic equations can be mapped to the ϕ^4 Landau-Ginzburg theory, and generically belong to the Ising universality class with conservative (model A) dynamics [39, 44?].

In conclusion, by using simulation and theoretical analysis, we study in detail the criticality of a minimal chemical reaction system. We find that increasing the reaction barrier effectively delays the transition but also increases the transition cooperativity which sharpens the transition. This cooperativity gain raised by the reaction barrier is different from that in the threshold contact process [10, 45], where the cooperativity is enforced by a topological property, i.e., the number of active neighbours. It is also different from the explosive percolation model which relies on information input to avoid the occurrence of the larger cluster [20–23]. In fact, the cooperativity in our chemical reaction system comes from the inertia of particles, which makes it possible for previous reactive collision to facilitate the consecutive ones. The cooperativity increases with raising the reaction barrier, as it demands more kinetic energy cumulation from previous collisions to trigger the consecutive ones. A similar memory-induced cooperativity controlled by a cumulation threshold have also been found in a contagion network model system [46]. Moreover, discontinuous dynamic phase transitions are found in glass-forming liquids [47–49], yielding of amorphous solids [50, 51] and high-density active matter systems [52, 53], where particles need to cross an energy barrier to make displacements. Therefore, our finding about the reaction barrier on the criticality of chemical reaction can not only help control the ignition in fuel engines and improve the chem-

ical storage safety, but also shed lights in the spread of epidemic, knowledge and innovations [54], as well as dynamic behaviours of amorphous materials.

This work has been supported in part by the Singapore Ministry of Education through the Academic Research Fund MOE2019-T2-2-010 and RG104/17 (S), by Nanyang Technological University Start-Up Grant (NTU-SUG: M4081781.120), by the Advanced Manufacturing and Engineering Young Individual Research Grant (A1784C0018) and by the Science and Engineering Research Council of Agency for Science, Technology and Research Singapore. We thank NSCC for granting computational resources.

* Electronic address: r.ni@ntu.edu.sg

- [1] Frank-Kamenetskii, D. A. *Diffusion and heat exchange in chemical kinetics* (Princeton University Press, 2015).
- [2] Semenov, N. Theories of combustion process. *Z. Phys. Chem.* **48**, 571–582 (1928).
- [3] Gray, B. Critical behaviour in chemically reacting systems: I Difficulties with the Semenov theory. *Combust. Flame* **20**, 313–316 (1973).
- [4] Gray, B. Critical behaviour in chemically reacting systems: II An exactly soluble model. *Combust. Flame* **20**, 317–325 (1973).
- [5] Shouman, A. R. A review of one aspect of the thermal-explosion theory. *J. Eng. Math.* **56**, 179–184 (2006).
- [6] Nowakowski, B. & Lemarchand, A. Stochastic effects in a thermochemical system with newtonian heat exchange. *Phys. Rev. E* **64**, 061108 (2001).
- [7] Nowakowski, B. & Lemarchand, A. Sensitivity of explosion to departure from partial equilibrium. *Phys. Rev. E* **68**, 031105 (2003).
- [8] Okoya, S. S. Disappearance of criticality in branched-chain thermal explosion with heat loss. Tech. rep., Abdus Salam International Centre for Theoretical Physics (2003).
- [9] Ebert, K. H., Deuffhard, P. & Jäger, W. *Modelling of Chemical Reaction Systems: Proceedings of an International Workshop, Heidelberg, Fed. Rep. of Germany, September 1–5, 1980*, vol. 18 (Springer Science & Business Media, 2012).
- [10] Schlögl, F. Chemical reaction models for non-equilibrium phase transitions. *Zeitschrift für physik* **253**, 147–161 (1972).
- [11] Claycomb, J., Bassler, K., Miller Jr, J., Nersesyan, M. & Luss, D. Avalanche behavior in the dynamics of chemical reactions. *Phys. Rev. Lett.* **87**, 178303 (2001).
- [12] Henkel, M., Hinrichsen, H. & Lübeck, S. *Non-equilibrium phase transitions: Absorbing Phase Transitions*, vol. 1 (Springer, 2008).
- [13] Grassberger, P. On phase transitions in Schlögl's second model. In *Nonlinear Phenomena in Chemical Dynamics*, 262–262 (Springer, 1981).
- [14] Tomé, T. & Dickman, R. Ziff-Gulari-Barshad model with CO desorption: An Ising-like nonequilibrium critical point. *Phys. Rev. E* **47**, 948 (1993).
- [15] Liu, D.-J., Pavlenko, N. & Evans, J. W. Crossover between mean-field and Ising critical behavior in a lattice-gas reaction-diffusion model. *J. Stat. Phys.* **114**, 101–114 (2004).
- [16] Bradley, D. How fast can we burn? In *Symposium (International) on Combustion*, vol. 24, 247–262 (Elsevier, 1992).
- [17] Griffiths, J. F. & Barnard, J. A. *Flame and combustion* (CRC Press, 1995).
- [18] Drysdale, D. *An introduction to fire dynamics* (John Wiley & Sons, 2011).
- [19] Cavaliere, A. & de Joannon, M. Mild combustion. *Prog. Energy Combust. Sci.* **30**, 329–366 (2004).
- [20] Achlioptas, D., D'Souza, R. M. & Spencer, J. Explosive percolation in random networks. *Science* **323**, 1453–1455 (2009).
- [21] da Costa, R. A., Dorogovtsev, S. N., Goltsev, A. V. & Mendes, J. F. F. Explosive percolation transition is actually continuous. *Phys. Rev. Lett.* **105**, 255701 (2010).
- [22] Riordan, O. & Warnke, L. Explosive percolation is continuous. *Science* **333**, 322–324 (2011).
- [23] Cho, Y. S., Hwang, S., Herrmann, H. J. & Kahng, B. Avoiding a spanning cluster in percolation models. *Science* **339**, 1185–1187 (2013).
- [24] DSouza, R. M. & Nagler, J. Anomalous critical and supercritical phenomena in explosive percolation. *Nat. Phys.* **11**, 531–538 (2015).
- [25] Manna, S. Two-state model of self-organized criticality. *J. Phys. A: Math. Gen.* **24**, L363 (1991).
- [26] Lei, Q.-L. & Ni, R. Hydrodynamics of random-organizing hyperuniform fluids. *Proc. Natl. Acad. Sci. U.S.A* **116**, 22983–22989 (2019).
- [27] Scala, A. Event-driven Langevin simulations of hard spheres. *Phys. Rev. E* **86**, 026709 (2012).
- [28] Rossi, M., Pastor-Satorras, R. & Vespignani, A. Universality class of absorbing phase transitions with a conserved field. *Phys. Rev. Lett.* **85**, 1803 (2000).
- [29] Boddington, T., Gray, P. & Robinson, C. Thermal explosions and the disappearance of criticality at small activation energies: exact results for the slab. *Proceedings of the Royal Society of London. A. Mathematical and Physical Sciences* **368**, 441–461 (1979).
- [30] Fenaughty, K., Lacey, A. & Wake, G. The disappearance of criticality for small activation energy with arbitrary Biot number. *Combust. Flame* **45**, 287–291 (1982).
- [31] Lacey, A. Critical behaviour of homogeneous reacting systems with large activation energy. *Int. J. Eng. Sci.* **21**, 501–515 (1983).
- [32] Lübeck, S. Tricritical directed percolation. *J Stat Phys* **123**, 193–221 (2006).
- [33] Janssen, H.-K., Müller, M. & Stenull, O. Generalized epidemic process and tricritical dynamic percolation. *Phys. Rev. E* **70**, 026114 (2004).
- [34] Araújo, N. A., Andrade Jr, J. S., Ziff, R. M. & Herrmann, H. J. Tricritical point in explosive percolation. *Phys. Rev. Lett.* **106**, 095703 (2011).
- [35] Lee, S. B. Comment on fixed-energy sandpiles belong generically to directed percolation. *Phys. Rev. Lett.* **110**, 159601 (2013).
- [36] di Santo, S., Burioni, R., Vezzani, A. & Muñoz, M. A. Self-organized bistability associated with first-order phase transitions. *Phys. Rev. Lett.* **116**, 240601 (2016).
- [37] Dornic, I., Chaté, H. & Munoz, M. A. Integration of Langevin equations with multiplicative noise and the viability of field theories for absorbing phase transitions.

- Phys. Rev. Lett.* **94**, 100601 (2005).
- [38] Dewel, G., Walgraef, D. & Borckmans, P. Renormalization group approach to chemical instabilities. *Zeitschrift für Physik B Condensed Matter* **28**, 235–237 (1977).
- [39] Brachet, M. & Tirapegui, E. On the critical behaviour of the Schlögl model. *Phys. Lett. A* **81**, 211–214 (1981).
- [40] Dewel, G., Borckmans, P. & Walgraef, D. Nonequilibrium phase transitions and chemical instabilities. *J. Stat. Phys.* **24**, 119–137 (1981).
- [41] Majdandzic, A. *et al.* Spontaneous recovery in dynamical networks. *Nat. Phys.* **10**, 34–38 (2014).
- [42] Böttcher, L., Nagler, J. & Herrmann, H. J. Critical behaviors in contagion dynamics. *Phys. Rev. Lett.* **118**, 088301 (2017).
- [43] Böttcher, L., Luković, M., Nagler, J., Havlin, S. & Herrmann, H. J. Failure and recovery in dynamical networks. *Sci. Rep.* **7**, 1–9 (2017).
- [44] Hohenberg, P. C. & Halperin, B. I. Theory of dynamic critical phenomena. *Rev. Mod. Phys.* **49**, 435 (1977).
- [45] Liu, D.-J., Guo, X. & Evans, J. W. Quadratic contact process: Phase separation with interface-orientation-dependent equistability. *Phys. Rev. Lett.* **98**, 050601 (2007).
- [46] Dodds, P. S. & Watts, D. J. Universal behavior in a generalized model of contagion. *Phys. Rev. Lett.* **92**, 218701 (2004).
- [47] Garrahan, J. P. *et al.* Dynamical first-order phase transition in kinetically constrained models of glasses. *Phys. Rev. Lett.* **98**, 195702 (2007).
- [48] Hedges, L. O., Jack, R. L., Garrahan, J. P. & Chandler, D. Dynamic order-disorder in atomistic models of structural glass formers. *Science* **323**, 1309–1313 (2009).
- [49] Speck, T., Malins, A. & Royall, C. P. First-order phase transition in a model glass former: Coupling of local structure and dynamics. *Phys. Rev. Lett* **109**, 195703 (2012).
- [50] Bonn, D., Denn, M. M., Berthier, L., Divoux, T. & Manneville, S. Yield stress materials in soft condensed matter. *Rev. Mod. Phys.* **89**, 035005 (2017).
- [51] Nagasawa, K., Miyazaki, K. & Kawasaki, T. Classification of the reversible–irreversible transitions in particle trajectories across the jamming transition point. *Soft matter* **15**, 7557–7566 (2019).
- [52] Tjhung, E. & Berthier, L. Discontinuous fluidization transition in time-correlated assemblies of actively deforming particles. *Phys. Rev. E* **96**, 050601 (2017).
- [53] Lei, Q.-L., Ciamarra, M. P. & Ni, R. Nonequilibrium strongly hyperuniform fluids of circle active particles with large local density fluctuations. *Sci. Adv.* **5**, eaau7423 (2019).
- [54] Pastor-Satorras, R., Castellano, C., Van Mieghem, P. & Vespignani, A. Epidemic processes in complex networks. *Rev. Mod. Phys.* **87**, 925 (2015).